ADVANCES IN ATMOSPHERIC SCIENCES, VOL. 28, NO. 3, 2011, 709–724

The Energy Budget of a Southwest Vortex With Heavy Rainfall over South China

FU Shenming* (傅慎明), SUN Jianhua (孙建华), ZHAO Sixiong (赵思雄), and LI Wanli (李万莉)

Institute of Atmospheric Physics, Chinese Academy of Sciences, Beijing 100029

(Received 9 February 2010; revised 28 May 2010)

ABSTRACT

Energy budgets were analyzed to study the development of an eastward propagating southwest vortex (SWV) associated with heavy rainfall over southern China (11–13 June 2008). The results show that kinetic energy (KE) generation and advection were the most important KE sources, while friction and sub-grid processes were the main KE sinks. There was downward conversion from divergent to rotational wind KE consistent with the downward stretching of SWVs. The Coriolis force was important for the formation and maintenance of the SWV. Convergence was also an important factor for maintenance, as was vertical motion during the mature stage of the SWV and the formation stage of a newly formed vortex (vortex B). The conversion from available potential energy (APE) to KE of divergent wind can lead to strong convection. Vertical motion influenced APE by dynamical and thermal processes which had opposite effects. The variation of APE was related to the heavy rainfall and convection; in this case, vertical motion with direct thermal circulation was the most important way in which APE was released, while latent heat release and vertical temperature advection were important for APE generation.

Key words: southwest vortex, kinetic energy, available potential energy

Citation: Fu, S. M., J. H. Sun, S. X. Zhao, and W. L. Li, 2011: The energy budget of a southwest vortex with heavy rainfall over South China. *Adv. Atmos. Sci.*, **28**(3), 709–724, doi: 10.1007/s00376-010-0026-z.

1. Introduction

The southwest vortex (SWV) over southwestern China is a mesoscale vortex with a horizontal scale of 200–600 km, and the main source areas of SWVs are located at (26°–34°N, 103°–110°E) (Fig. 1). The cyclonic circulation of SWVs mainly appears in the lower troposphere (700 hPa and below). Owing to the complex topography of the Tibetan Plateau and Sichuan Basin (Fig. 1), the isohypse is sometimes unable to close. Thus, stream fields are often analyzed in studies of SWVs (Lu, 1986; Zhao and Fu, 2007; Fu, 2009). The SWV is one of the most important heavy rainfall systems over eastern parts of China (Tao, 1980; Lu, 1986; Chen et al., 2003), and occurs frequently in summer and autumn (Chen and Min, 2000; Chen et al., 2007). Many previous studies (Lu, 1986; Gao, 1987; Sun and Chen, 1994; Chen and Min, 2000; Chen et al., 2007; Zhao and Fu, 2007; Fu, 2009) have shown that the generation of SWVs is related to topographic effects from the Tibetan Plateau and Sichuan Basin, as well as the presence of favorable synoptic circulations. The structure of the SWV differs from extratropical and tropical cyclones (Zhao, 1977; Zhao and Fu, 2007; Lu, 1986; Chen et al., 1998). There are many contributions in the literatures to study the statistical features and main sources of SWVs (Chen and Min, 2000; Chen et al., 2007), their formation and development mechanisms (Gao, 1987; Wu and Liu, 1999; Li et al., 2002; Zhu et al., 2002), as well as numerical simulation of SWVs and associated heavy rainfall (Chen and Lorenzo, 1984; Kuo et al., 1988; Wang and Gao, 2003). However, the energy budgets associated with the development of SWVs has not been analyzed.

Energy budget analysis is a useful tool in process studies, and has been widely used in studies of cyclones. The analysis of kinetic energy (KE) budgets have been applied to study the effects of divergent and non-divergent winds on the KE budget of atmospheric circulations and a mid-latitude cyclone (Chen and Wiin-Nielsen, 1976; Chen et al., 1978), the energy exchange between meso- and synoptic-scale cir-

*Corresponding author: FU Shenming, fusm@mail.iap.ac.cn

culations (Chen et al., 1990), as well as between the divergent and rotational components of atmospheric flows over the tropics and subtropics at 200 hPa (Chen, 1980), and the KE budget of a typhoon (Ding and Liu, 1985a, b). For an isolated system, available potential energy (APE) is the sole source of KE (Chen and Wiin-Nielsen, 1976; Ding and Liu, 1985a, b), and serves as an important energy source for atmospheric circulations in the extratropics (Chen et al., 1978; Ding and Liu, 1985a, b). APE is transferred to the KE associated with divergent winds, which in turn is transferred into the KE of rotational winds during the development of cyclones. Edmon (1978) developed a new equation for APE. Lorenz (1978) used the APE budget to study the maintenance of a moist circulation. The APE budget of a typhoon and the relationship between APE and typhoon heavy rainfall have also been analyzed (Ding and Liu, 1985a, b; Ding and Chen, 1995). The effects of temperature advection on APE have been studied during a heavy rainfall event (Zhao and Fu, 2007).

In this paper, the KE and APE budgets are calculated to study the mechanisms associated with the development of an eastward-propagating SWV over southern China during 11–13 June 2008 and its relationship with heavy rainfall. The data and methodology are discussed in the next section. The evolution of the SWV and its associated heavy rainfall are analyzed in section 3, and the budget analysis is presented in section 4. A summary and conclusions are given in section 5.

2. Data and methodology

Final analysis data (four times daily) with a horizontal resolution of 1°×1° from the NCEP (National Centers for Environmental Prediction) were used to calculate the energy budget. Conventional surface and sounding observations, intensified observations from SCHeREX (South China Heavy Rainfall Experiment) and hourly TBB (temperature of black body) data from Satellite Fengyun (FY)-2C with a resolution of 0.1°×0.1° were also used to investigate the evolution of heavy rainfall and the SWV.

2.1 *KE budget*

KE associated with both rotational and divergent winds are important (Lu, 1986; Zhao and Fu, 2007; Fu, 2009) in SWVs. The KE budget equation used in the present study was sourced from Chen et al. (1978):

$$\frac{\delta k}{\delta t} = -J(\psi, k) + \nabla_{\rm h}\chi \cdot \nabla_{\rm h} k - \omega\frac{\partial k}{\partial p} + \boldsymbol{C} \cdot \nabla_{\rm h} k - J(\psi, \phi) + \nabla_{\rm h}\chi \cdot \nabla_{\rm h}\phi + \boldsymbol{V}_{\rm h} \cdot \boldsymbol{F} \quad (1)$$

where the subscript "h" stand for horizontal. Integrating Eq. (1) in an air column leads to the KE equation used by Dimego and Bosart (1982) and Ding and Liu

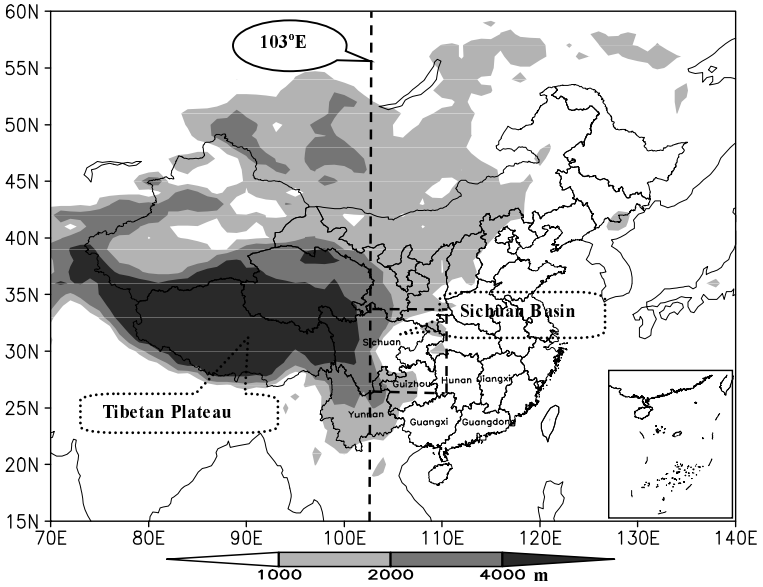

Fig. 1. The orography of the Tibetan Plateau (height above 1000 m is shaded). The thick dashed line is the east boundary line (103°E) of the Tibetan Plateau, and the dashed rectangle represents the SWV source area.

(1985a):

$$\frac{\delta K}{\delta t} = \frac{1}{g}\int_{p_u}^{p_b}\left[-\overline{\overline{J(\psi,k)}}+\overline{\overline{\boldsymbol{C}\cdot\nabla k}}-\frac{l}{S}\overbrace{kv_{\chi^a}}-\frac{\partial\overline{\overline{\omega k}}}{\partial p}\right]dp+\frac{1}{g}\int_{p_u}^{p_b}\left[-\overline{\overline{J(\psi,\phi)}}+\overline{\overline{\nabla\chi\cdot\nabla\phi}}\right]dp+D(k)\ . \tag{2}$$

OB NFC SFC DFC VFC NG DG RES

In Eqs. (1) and (2), $\delta/\delta t$ represents Lagrange variation, and k stands for horizontal kinetic energy per unit mass. K is the volume integral (integrated in an air column containing the vortex) of k, ψ the stream function, and χ the potential function, which in this study were calculated using the successive relaxation method, $J(\ )$ the Jacobi operator, g the gravity acceleration rate, $\boldsymbol{C}$ the horizontal velocity vector of research object, ϕ the geopotential, $\boldsymbol{F}$ the friction force per unit mass, S the area of horizontal integral, l the boundary line of area S, $v_{\chi a}$ the velocity component along the normal direction of the boundary line, p_b the pressure at the lowest level of the air column, $D(k)$ the residual term, and p_u the pressure at the highest level of the air column. $\overline{\overline{(\ )}}=\frac{1}{S}\int_s(\ )dS$ represents the area integral and $\overbrace{(\ )}=\frac{1}{l}\int_l(\ )dl$ stands for the curvilinear integral.

In Eq. (2), OB stands for the KE Lagrange variation, NFC is the KE advection by rotational wind, SFC is the advection caused by system movement, DFC is the KE advection by divergent wind, VFC is the vertical advection associated with vertical motion, NG is the KE generation caused by rotational wind, DG is the KE generation by divergent wind, and RES is the effect of friction and sub-grid processes, which can be calculated by the residual, i.e. RES=OB−(NFC+SFC+DFC+VFC+NG+DG).

Equations (3)–(5) were used by Chen et al. (1978) and (Ding and Liu, 1985a,b). Since the SWV is a kind of strong mesoscale vortex, rotational and divergent winds are very important (Lu, 1986; Zhao and Fu, 2007; Fu, 2009). Here, the KE associated with the rotational and divergent winds can be written by:

$$\frac{\partial K_\psi}{\partial t} = B_\psi + H(K_\chi, K_\psi) + F_\psi\ , \tag{3}$$

$$\frac{\partial K_\chi}{\partial t} = B_\chi + H(P, K_\chi) - H(K_\chi, K_\psi) + F_\chi\ , \tag{4}$$

$$\frac{\partial (P+I)}{\partial t} = B_{P+I} - H(P, K_\chi) + Q_{P+I} + F_T\ . \tag{5}$$

In Eqs. (3)–(5), K_ψ stands for rotational wind KE, K_χ is divergent wind KE, $P+I$ is the total potential energy, where P is the potential energy and I is internal energy. B_ψ,B_χ,B_{P+I} are the boundary fluxes, F_ψ, F_χ, F_T are the friction terms of Eqs. (3)–(5) respectively, where the subscripts are used to make distinctions among them, and Q_{P+I} is the diabatic heating term.

$$H(K_\chi, K_\psi) = f\nabla_h\chi\nabla_h\psi+\nabla_h^2\psi\nabla_h\chi\cdot\nabla_h\psi+\frac{|\nabla_h\psi|^2}{2}\nabla_h^2\chi+\omega J\left(\psi,\frac{\partial\chi}{\partial p}\right)\ . \tag{6}$$

SP Sp1 Sp2 Sp3 Sp4

Equation (6) is the conversion between divergent wind KE and rotational wind KE, which is defined as SP. SP contains four terms: Sp1 represents the following vorticity term; Sp2 is the relative vorticity term; and Sp3 and Sp4 are the divergence and vertical motion terms, respectively. For the Northern Hemisphere, the Coriolis parameter $f>0$, and the vorticity of cyclones is positive, which means $\nabla_h^2\psi>0$. When the angle between $\nabla_h\psi$ and $\nabla_h\chi$ is less than 90°, it is given that Sp1>0, Sp2>0, which means divergent wind KE is converted to rotational wind KE, which is favorable for the development of a cyclone. When $\nabla_h\psi$ is perpendicular to $\nabla_h\chi$, there is no conversion via Sp1 and Sp2. Sp3 shows that the convergence causes conversion of KE from the divergent wind to the rotational wind. Sp4 can be rewritten as

$$\omega J(\psi,\frac{\partial\chi}{\partial p}) = -\omega\left(-\boldsymbol{V}_\psi\cdot\nabla\frac{\partial\chi}{\partial p}\right)\ ,$$

where $\boldsymbol{V}_\psi$ is the rotational wind vector. In regions with an ascending motion, if the rotational wind moves along $-\nabla\partial\chi/\partial p$, the divergent wind converts to the rotational wind. While in the regions with a descending motion, if rotational wind moves along $\nabla\partial\chi/\partial p$, the divergent wind converts to the rotational wind. In Eqs. (4) and (5), $H(P,K_\chi)=-\chi\nabla_h^2\phi$ (CAD) stands for the conversion between APE and divergent wind KE. For a cyclone, the geopotential is a concave function, in which the sign of CAD is determined by the

sign of the potential function for $\nabla_{\rm h}^2\phi > 0$. In regions with $\chi < 0$, APE is converted to divergent wind KE (this will be elucidated in the following discussions).

2.2 *APE budget*

Since there is always heavy rainfall associated with SWVs, there are ascending motions and associated strong latent heat release, which may impact upon the variation of APE. APE is the part of total potential energy which could be converted to KE and is defined as

$$A = \frac{c_p}{\sigma g}\int_{\sigma}\int_{p_{\rm u}}^{p_{\rm s}} NT dpdxdy\ ,$$

where N represents the efficiency factor, c_p the specific heat at constant pressure, σ the integral area, $p_{\rm s}$ the surface pressure, $p_{\rm u}$ the top level pressure, and T the temperature.

Edmon (1978) derived an APE budget equation, in which the terms of the equation have similar orders of magnitude:

$$\underbrace{\frac{\partial A}{\partial t}}_{} = \underbrace{\frac{1}{\sigma g}\int_{\sigma}\int_{p_{\rm u}}^{p_{\rm s}} NQdpds}_{\rm A1} + \underbrace{\frac{1}{\sigma g}\int_{\sigma}\int_{p_{\rm u}}^{p_{\rm s}} N\omega\alpha dpds}_{\rm A2} - \underbrace{\frac{c_p}{\sigma g}\int_{\sigma}\int_{p_{\rm u}}^{p_{\rm s}} N\boldsymbol{V}\cdot\nabla_{\rm p}Tdpds}_{\rm A3} - \underbrace{\frac{c_p}{\sigma g}\int_{\sigma}\int_{p_{\rm u}}^{p_{\rm s}} N\omega\frac{\partial T}{\partial p}dpds}_{\rm A4}$$

$$+\underbrace{\frac{c_p}{\sigma g}\int_{\sigma}\int_{p_{\rm u}}^{p_{\rm s}} T\frac{\partial N}{\partial t}dpds}_{\rm A5} + \underbrace{\frac{c_p}{\sigma g}\int_{\sigma} N_{\rm s}T_{\rm s}\frac{\partial p_{\rm s}}{\partial t}ds}_{\rm A6}\ . \tag{7}$$

In Eq. (7), Q stands for diabatic heating, $N_{\rm s}$ the efficiency factor at surface, $T_{\rm s}$ surface temperature, and $p_{\rm s}$ the surface pressure. A1 is APE generation from diabatic heating, A2 is APE variation affected by vertical motion (dynamical process), A3 is APE variation due to temperature advection (thermal process), A4 is APE generation related with vertical temperature advection, A5 is APE variation caused by efficiency factor variation, and A6 is APE variation by surface effects.

We defined a1= NQ; a2= $N\omega\alpha$; a3= $c_pN(-\boldsymbol{V}\cdot\nabla_{\rm p}T)$; and a4= $c_pN[-\omega(\partial T/\partial p)]$. These four terms correspond to terms A1–A4 and they are calculated to investigate the relationship between heavy rainfall and the SWV. In the present paper, only moisture latent heat release is considered in Q (sensible heat and radiation heating have also been calculated, however latent heat is much more than these two terms), and it was calculated using the Kuo scheme (Kuo, 1974). The calculation results with the Kuo scheme can approximately represent the rainfall distribution (not shown), and can be used to clarify the effects of diabatic heating on APE variation qualitatively.

3. Evolution of the SWV and heavy rainfall

At 1800 UTC 10 June 2008, there was strong horizontal cyclonic wind shear at 700 hPa, and six hours later (0000 UTC 11 June) a SWV formed in southern Sichuan (Fig. 2). The SWV moved southeastward and then turned northeastward at 1200 UTC 12 June, before dying out at 700 hPa at 0000 UTC 13 June. While the SWV was still maintained at 850 hPa (not shown), it completely dissipated six hours later. At 0000 UTC 13 June, a new vortex, named "vortex B", formed to the northeast of the SWV (Fig. 2). Based on the vorticity and streamline, the SWV life cycle can be divided into three stages: the formation stage (from 1800 UTC 10 to 0000 UTC 11 June 2008), the maintenance stage (including the mature stage, from 0600 UTC 11 to 1200 UTC 12 June 2008), and the dissipating stage (including the formation stage of vortex B, from 1800 UTC 12 to 0000 UTC 13 June 2008). Key areas (KA) of the SWV are shown in Fig. 2, and the evolution of the SWV is specified in Table 1.

The SWV lasted for about 54 hours, with a maximum horizontal scale of about 600 km (meso-α scale). The maximum hourly precipitation amount was about 90 mm, and the maximum total precipitation amount was above 250 mm over the northeast of Guangxi. At 1800 UTC 10 June (six hours before the formation of the SWV), there was strong convection in the southern part of Sichuan (Fig. 3). The convection was caused by horizontal wind shear, while the latent heat release was favorable for the formation of the SWV. During the lifetime of the SWV, the convective clouds moved along with the SWV with the TBB center below -72°C. It is found that intense convection often occurs in the central, southern and eastern parts of the SWV and most of the heavy rainfall episodes occurred

during the period 0000 UTC to 1200 UTC 12 June (Fig. 3).

4. Analysis of KE and APE

4.1 *KE budget results*

4.1.1 *Integrated KE budget of SWV*

As shown in Table 1, the vertical structures of the SWV evolved differently. Thus, we conducted vertical integrations in different levels at different times (Fig. 4). The term OB had three periods of positive and two periods of negative values during the lifetime of the SWV. Favorable for the formation of the SWV, KE in KAs increased beforehand. KE decreased at 0000 UTC 11 June when the SWV was formed. This was associated with a sudden decrease of VFC; that is, vertical motion transported KE out of the SWV levels, and the SWV developed slowly in the incipient maintenance stage. Term OB reached a maximum at 0000 UTC 12 June, and at the same time the terms SFC and VFC also reached a peak. The KE decreased rapidly, while the term SFC became negative. KE of the KA increased again at 0000 UTC 13 June when vortex B formed.

From the term NFC (rotational wind KE advection), it mainly had non-positive effects on the growth of KE, except for at 0000 UTC 12 and 0000 UTC 13 June. The NFC reached a maximum when vortex B formed. The term DFC (divergent wind KE advection) had slight positive effects on KE, which was favorable for the increase of KE. The term SFC had a positive effect on the increase of SWV KE. When the SWV moved southeastward, it remained positive (except for at 1200 UTC 11 June), and when the SWV moved northeastward, it changed to negative. From the distribution of KE (not shown), it was found that the KE of the SWV increased when the SWV moved from weak wind KE areas to strong wind KE areas, and vice versa. This indicates that the KE distribution of the background circulation was very important to the development of the SWV.

From the aforementioned analyses, the total effect of horizontal advection, NFC+ DFC+ SFC, was very important when the SWV was near the mature stage and vortex B formed. The term VFC (vertical KE advection) was unfavorable for incipient development of the SWV, but was favorable for maintenance of the SWV during the maintenance and dissipating periods. However, it was not favorable for the formation of vortex B. The term NFC+DFC+SFC+VFC can be seen as the effect of background circulation (friction and turbulence effects were neglected), and the total effect of the above four terms is shown in Fig. 4. The background circulation had negative effects on the increase in SWV KE during the incipient development stage, and played the most important role in maintaining SWV KE during the SWV mature stage. However, the background was slightly unfavorable for maintenance of the SWV in the SWV dissipating stage, while it was

Table 1. Evolution characteristics of the SWV.

Stages of the SWV	Time	KA of the SWV	Vertical distribution of the SWV
Formation stage	1800 UTC 10 June	KA1: 25°–29°N, 101°–106°E	Low level convergence (LLC), high level divergence (HLD), with strong vertical motion, no SWV
	0000 UTC 11 June	KA1: 25°–29°N, 101°–106°E	LLC and HLD with strong vertical motion, SWV locates in 550–750 hPa
Maintenance stage	0600 UTC 11 June	KA2: 25°–28.5°N, 101°–105.5°E	LLC and HLD with strong vertical motion, SWV locates in 550–750 hPa
	1200 UTC 11 June	KA3: 24°–28°N, 101.5°–105.5°E	LLC and HLD, vertical motion became stronger, SWV locates in 550–750 hPa
	1800 UTC 11 June	KA4: 24°–28°N, 102°–106.5°E	LLC and HLD, vertical motion weakened, SWV locates in 550–750 hPa
Mature stage	0000 UTC 12 June	KA5: 23.5°–28°N, 102.5°–109°E	LLC and HLD became weak, vertical motion weakend, SWV locates in 550–800 hPa
	0600 UTC 12 June	KA6: 22.5°–27.5°N, 103.5°–111°E	LLC became strong, HLD and vertical motion kept weak, SWV locates in 600–850 hPa
	1200 UTC 12 June	KA7: 23°–28°N, 105°–111.5°E	LLC and HLD became strong, with intense vertical motion, SWV locates in 550–900 hPa
Dissipating stage of SWV	1800 UTC 12 June	KA8: 23°–29°N, 106°–113°E	LLC, HLD and vertical motion became weak, SWV locates in 600–900 hPa
Formation stage of vortex B	0000 UTC 13 June	KA9: 25°–31°N, 110°–117°E	LLC and HLD became strong, with intense vertical motion, SWV locates at around 850 hPa

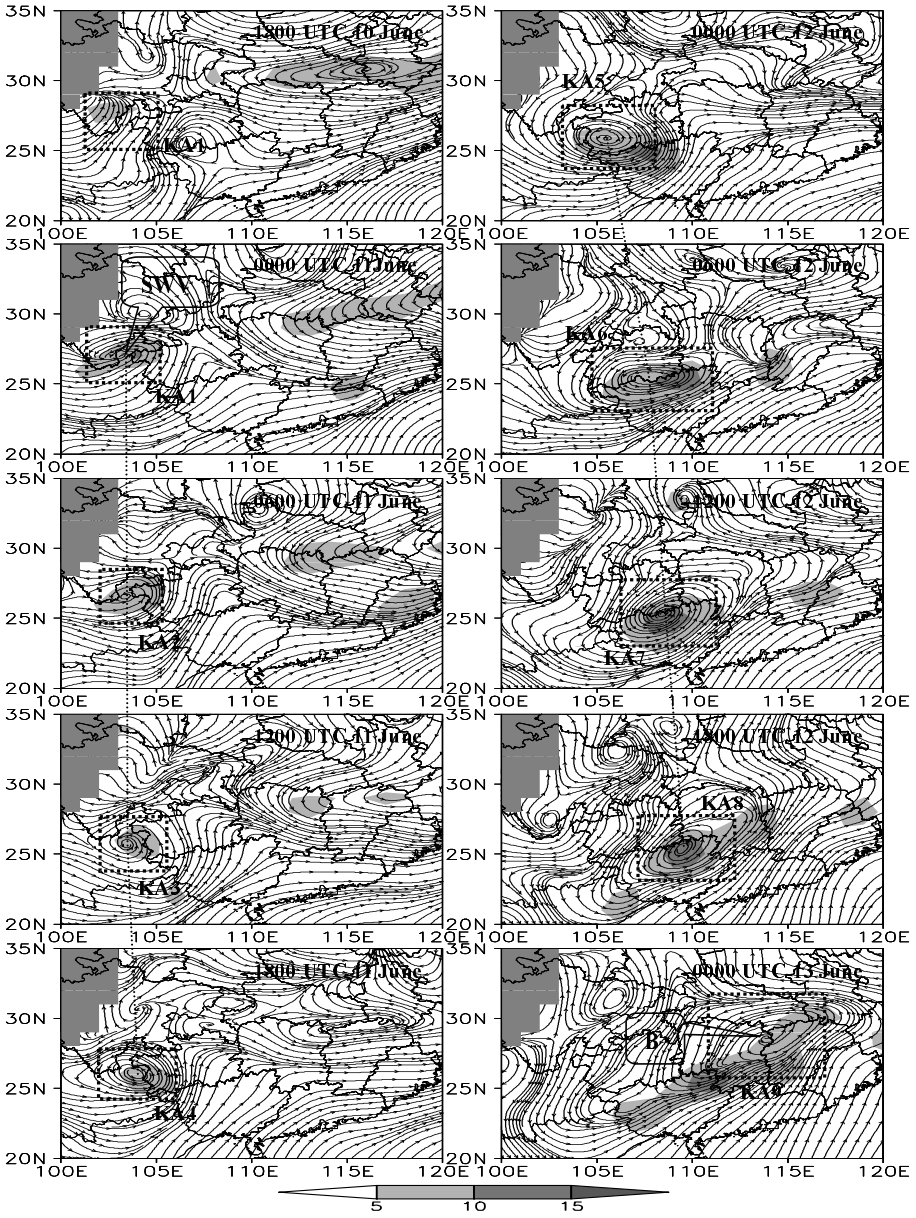

Fig. 2. Streamline at 700 hPa during heavy rainfall in Guangxi. Shading represents vorticity (10^{-5} s^{-1}), terrain above 3000 m is shaded grey, dotted rectangles are key areas (KAs) of the SWV, and dotted lines represent the direction of movement of the SWV.

advantageous to the formation of vortex B.

Both NG (rotational wind KE generation) and DG (divergent wind KE generation) reached their maxima at 1800 UTC 10 June (six hours before the formation of the SWV), which was favorable for the formation of the SWV, and then decreased rapidly. It is worth noting that the term NG maintained positive effects on the increase in SWV KE and had large positive values during the SWV dissipating stage, which was favorable for the maintenance of the SWV. The term DG showed positive values, except for at 0600 UTC and 1800 UTC 12 June. From the total effects of the terms NG and DG (Fig. 4), it is revealed that NG and DG played the most important roles in the formation and incipient maintenance stages of the SWV, and they were the most important KE sources during the SWV decaying stage. Compared to KE generation with KE advection, they were nearly as important, although the relative importance was different during different stages. KE generation was more important in the SWV incipient maintenance and decay stages than in the other stages, while KE advection was more

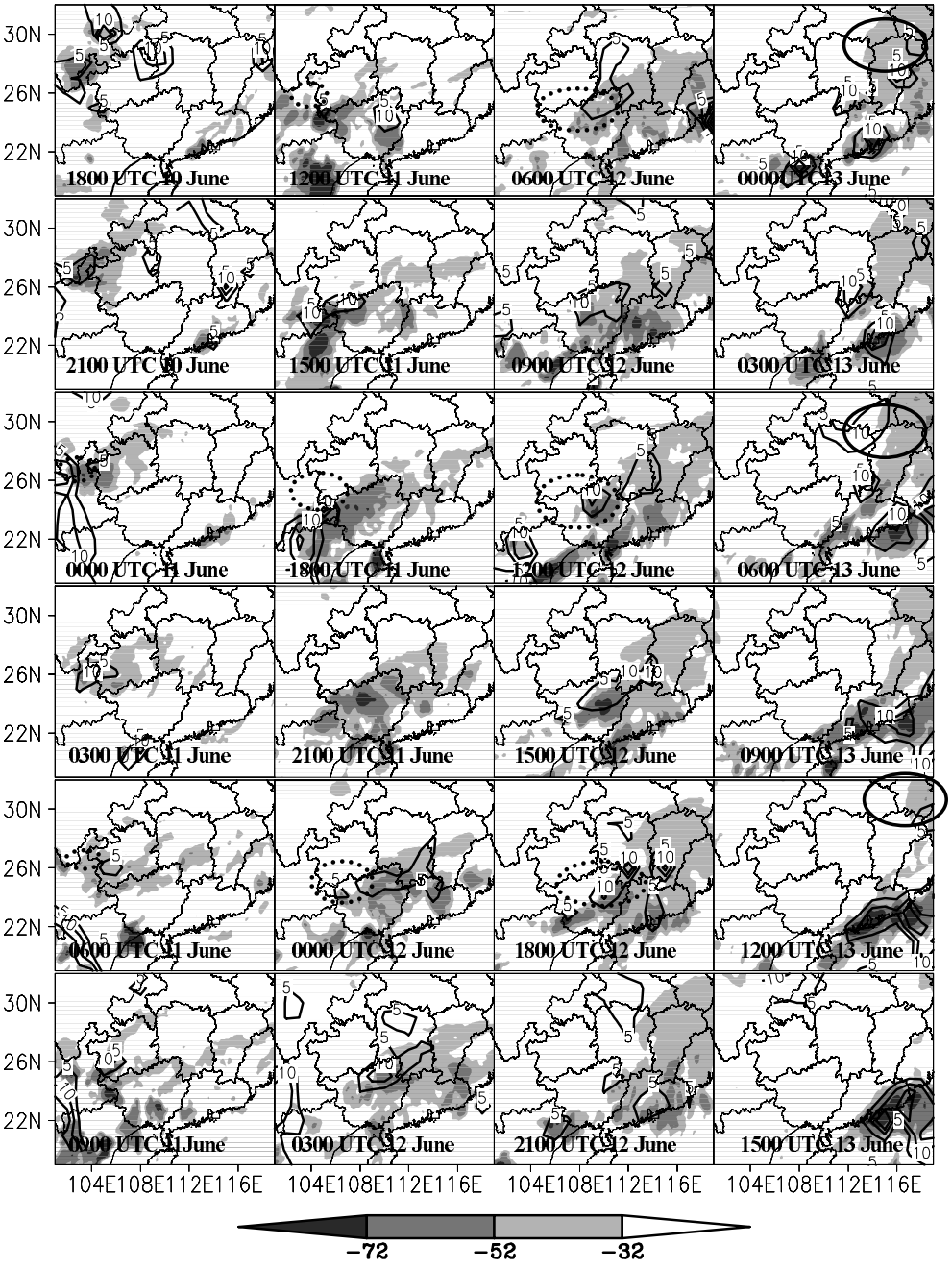

Fig. 3. The development of TBB (shaded, units: °C) and hourly precipitation amount (solid, units: mm). Dotted ellipses stand for the SWV, and solid ellipses represent vortex B.

important during the SWV middle maintenance stage and the formation of vortex B. Form the above analysis, the SWV was formed through KE generation, while vortex B was formed through KE advection.

Next, the term TOTAL is defined as TOTAL =NFC+ DFC+ SFC+ VFC+ NG+DG, which indicates the total effects of KE generation and KE advection. TOTAL remained positive during the entire lifetime of the SWV (Fig. 4). The three maximums occurred six hours before formation of the SWV, six hours before the SWV mature stage, and six hours before the formation of vortex B. Comparing TOTAL to the term RES, the term RES remained negative, except for at 1800 UTC 12 June. The implication is that friction and sub-grid processes were the most important SWV KE sinks, varying in an almost trend to the term TOTAL.

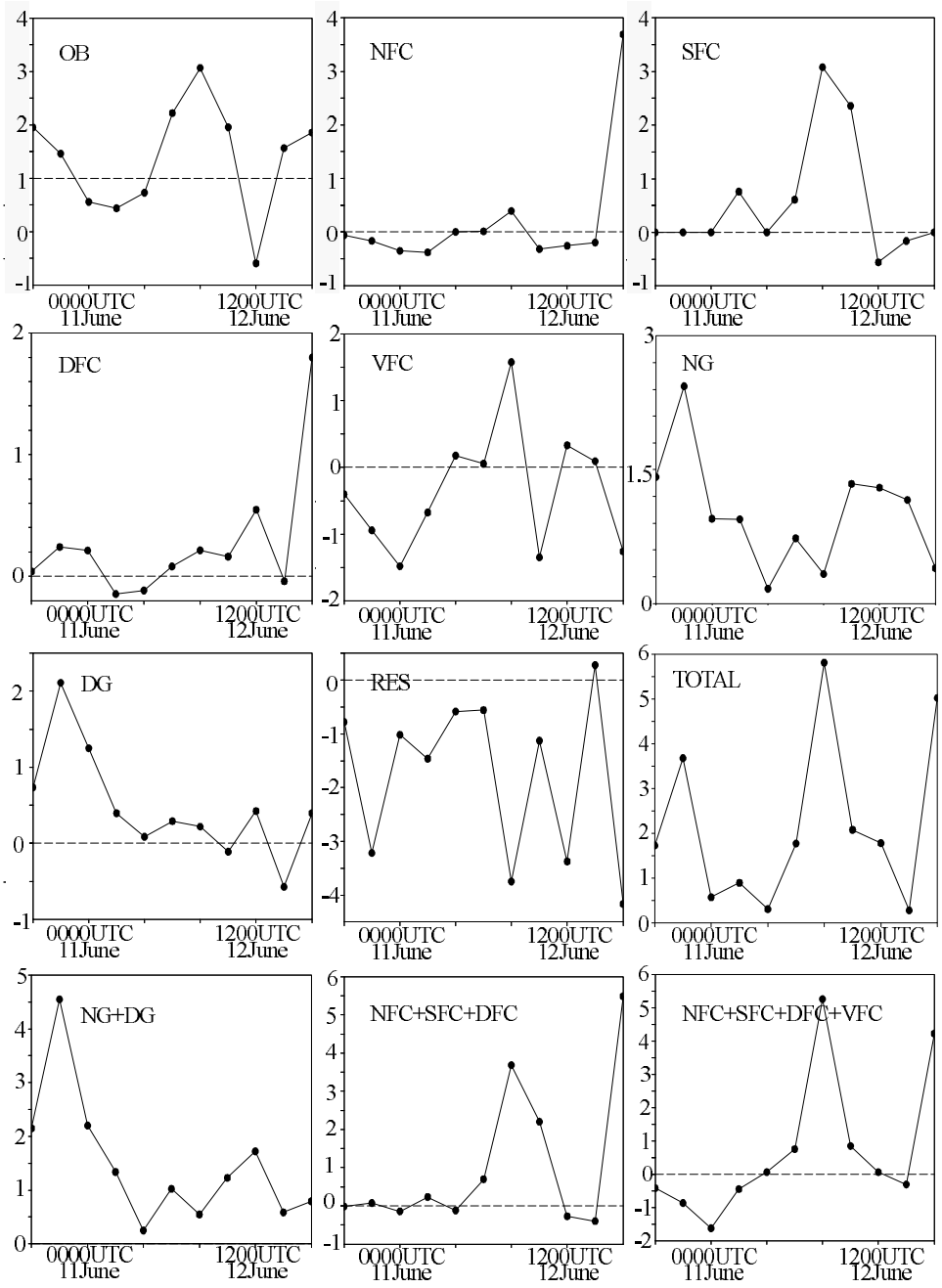

Fig. 4. Variations in each of the terms of the KE budget in the SWV KAs from 1200 UTC 12 to 0000 UTC 13 June 2008 (units: J m^{-2} s^{-1}).

4.1.2 *The conversion between rotational and divergent wind KE*

The conversion between rotational and divergent wind KE was calculated using the method shown in section 2.1 (term SP). The SWV appeared below 450 hPa (Table 1), so only the middle and low-levels are shown in Fig. 5. The maximum of term SP moved downward gradually, corresponding to the SWV stretching from the mid to lower troposphere (Table 1). Term Sp1 was the most important positive term before the formation of the SWV. This implies that the Coriolis force was essential to the formation of the SWV, as in the formation of extratropical cyclones. At the same time, the terms Sp2 and Sp3 were slightly positive, associated with the cyclonic wind shear and convergence, while the vertical motion term (Sp4) was negative, which was unfavorable for the formation of

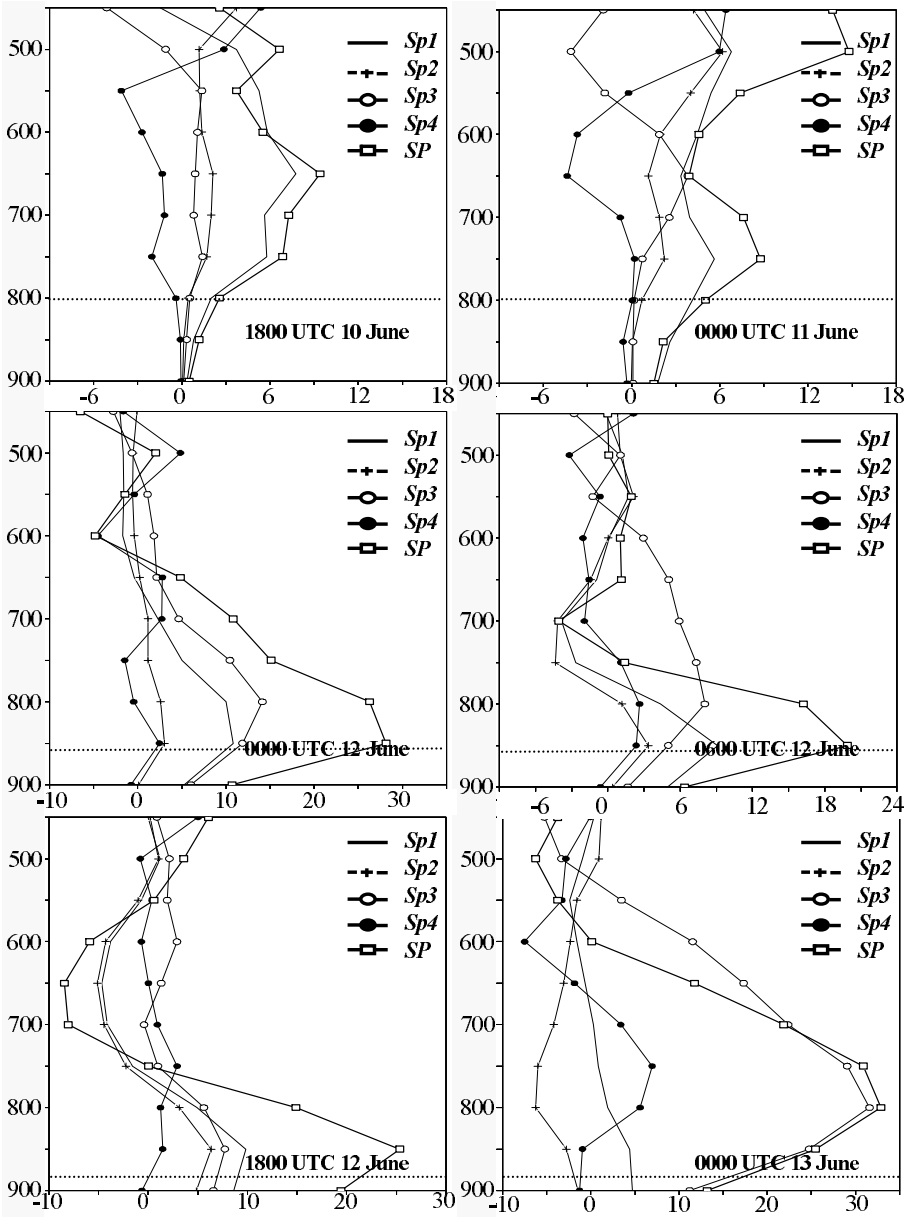

Fig. 5. Conversion terms of area-averaged rotational and divergent wind KE (solid, units: 10^{-4} J kg^{-1} s^{-1}) in KAs of the SWV. Dotted lines stand for the representative terrain height in the SWV KAs.

the SWV. When the SWV formed at 0000 UTC 11 June, the convergence intensified and the divergence term (Sp3) became important, with a maximum at 650 hPa. The term Sp1 decreased, but was still the most important term, indicating the Coriolis force was very important for the incipient maintenance of the SWV. The term Sp2 remained slightly positive, and vertical motion (Sp4) was unfavorable for the maintenance of the SWV.

In the mature stage of the SWV, the strongest vortex level was located approximately at 850 hPa. The terms Sp3 and Sp1 were the most important for the maintenance of the SWV. The vorticity term (Sp2) was favorable for the maintenance of the SWV at lower levels, and the term Sp4 (vertical motion) began to be favorable to the maintenance of the SWV. At 0600 UTC 12 June, the term SP changed to negative, indicating a weakening of the SWV at 700 hPa (Fig. 2).

In the dissipating stage of the SWV, at 1800 UTC 12 June, the term SP reached a negative maximum at 650 hPa. However, it remained positive with maximum values at 850 hPa, indicating that the SWV de-

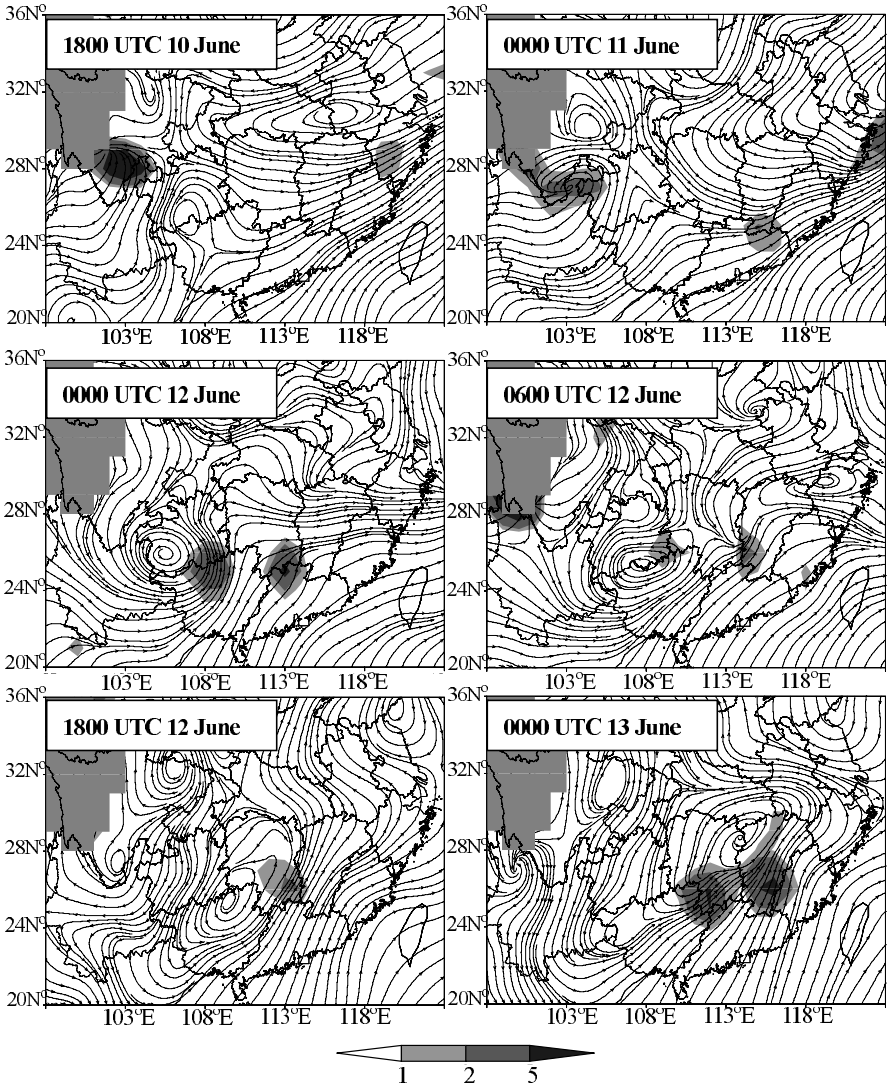

Fig. 6. The conversion from APE to divergent wind KE at 700 hPa (shaded, units: 10^{-3} J kg^{-1} s^{-1}). Solid lines are streamlines at 700 hPa and terrain above 3000 m is shaded grey.

cayed first in the middle troposphere (also shown in Table 1). The terms Sp1–Sp4 all remained positive at the lower levels, which was favorable for the maintenance of the SWV (Fig. 5). When vortex B formed, the term Sp3 (associated with convergence) was the most important term. This demonstrates that advection by the background circulation was the most important factor in the formation of vortex B. The vertical motion and Coriolis force were also favorable for the formation of vortex B.

4.1.3 *The conversion between APE and divergent wind KE*

Since APE is the source of KE, the conversion between APE and KE associated with divergent winds was calculated using the method shown in section 2.1 (term CAD). It is worth noting that the positive centers of term CAD (in KAs) were consistent with the intense convective activity, indicating that convection is related to the release of APE.

There was a strong positive CAD center in the KA 16 hours before the formation of the SWV corresponding to the term DG maximum in Fig. 6, which was favorable for the formation of the SWV. Also, there was a negative potential function (Fig. 7), a strong upward motion, and severe convergence centers corresponding to the CAD center, indicating that the conversion from APE to divergent wind KE reinforced the convergence in KA1 and upward motion. The averaged conversion from APE to divergent wind KE in KAs shows that

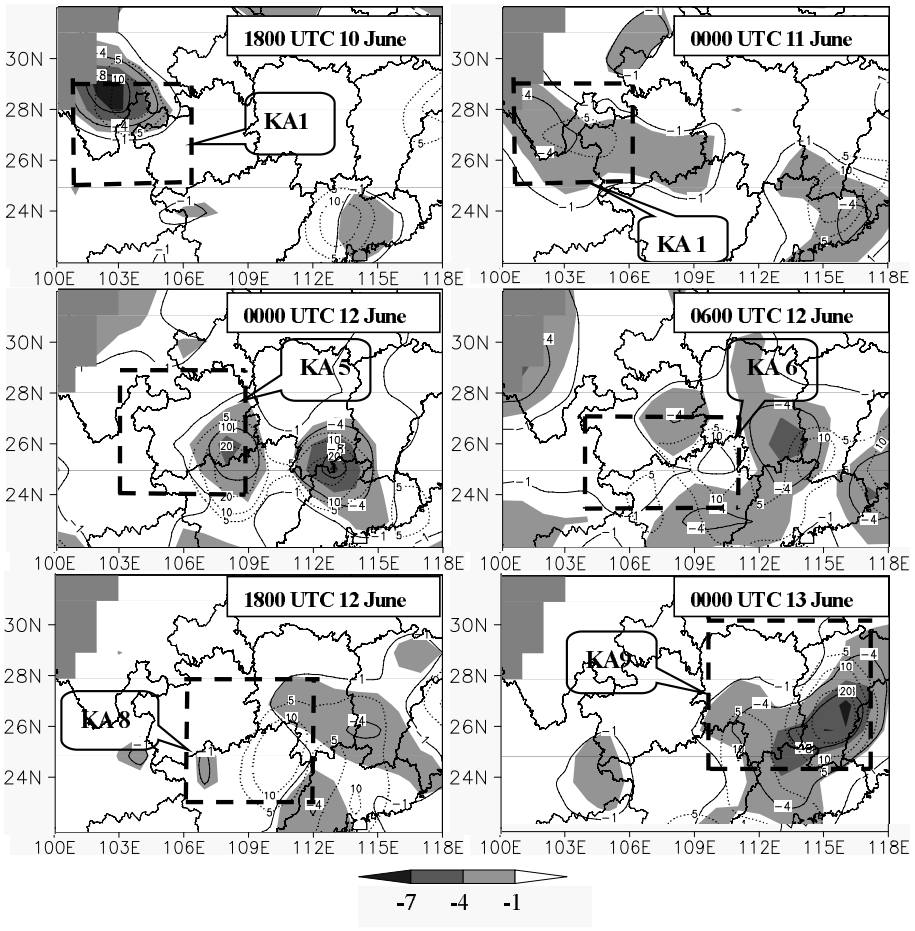

Fig. 7. The distribution of the potential function at 700 hPa (solid, only negative values are marked, units: 10^5 m^2 s^{-1}). Shaded areas represent convergence (units: 10^{-5} s^{-1}), dotted lines stand for vertical velocity (only positive values are marked, units: 10^{-2} m s^{-1}), dashed rectangles represent KAs of the SWV, and terrain above 3000 m is shaded grey.

APE was converted to divergent wind KE below 500 hPa (Fig. 8). There was a maximum around 750 hPa, which was the most important energy source for the formation of the SWV. At 0000 UTC 11 June, the formation stage of the SWV, the positive center of the term CAD and the corresponding negative potential function, upward motion, and convergence centers became weaker, but still remained strong in KA1. Figure 8 shows that the conversion from APE to divergent wind KE became weak around 700 hPa, but intensified at 500 hPa.

In the mature stage of the SWV (Fig. 6), there were positive centers of the term CAD in the SWV KAs, corresponding to the convective activity in the eastern SWV (Fig. 3), and the conversion became weak at 0600 UTC 12 June. This suggests that the negative potential function, upward motion, and convergence centers were in accordance with the conversion centers in the SWV KAs, and they all became weak at 0600 UTC 12 June. The term CAD remained positive below 550 hPa in the SWV KAs (Fig. 8), which was favorable for the maintenance of the SWV. The maximums of the term CAD, as well as SP (Fig. 5), moved from the mid to the lower troposphere, and conversion at 700 hPa became weak.

In the dissipating stage of the SWV, there was a positive center of the term CAD to the northeast of the SWV KA, and the corresponding convergence and negative potential function became weak. Upward motion (convection) still remained strong for the maintenance of the SWV (Fig. 5). The term CAD became negative around 700 hPa (Fig. 8), corresponding to the negative SP term (Fig. 5) and indicating that the SWV decayed at 700 hPa. Meanwhile, the terms SP and CAD were positive around 850 hPa, which was favorable for the maintenance of the SWV in the lower

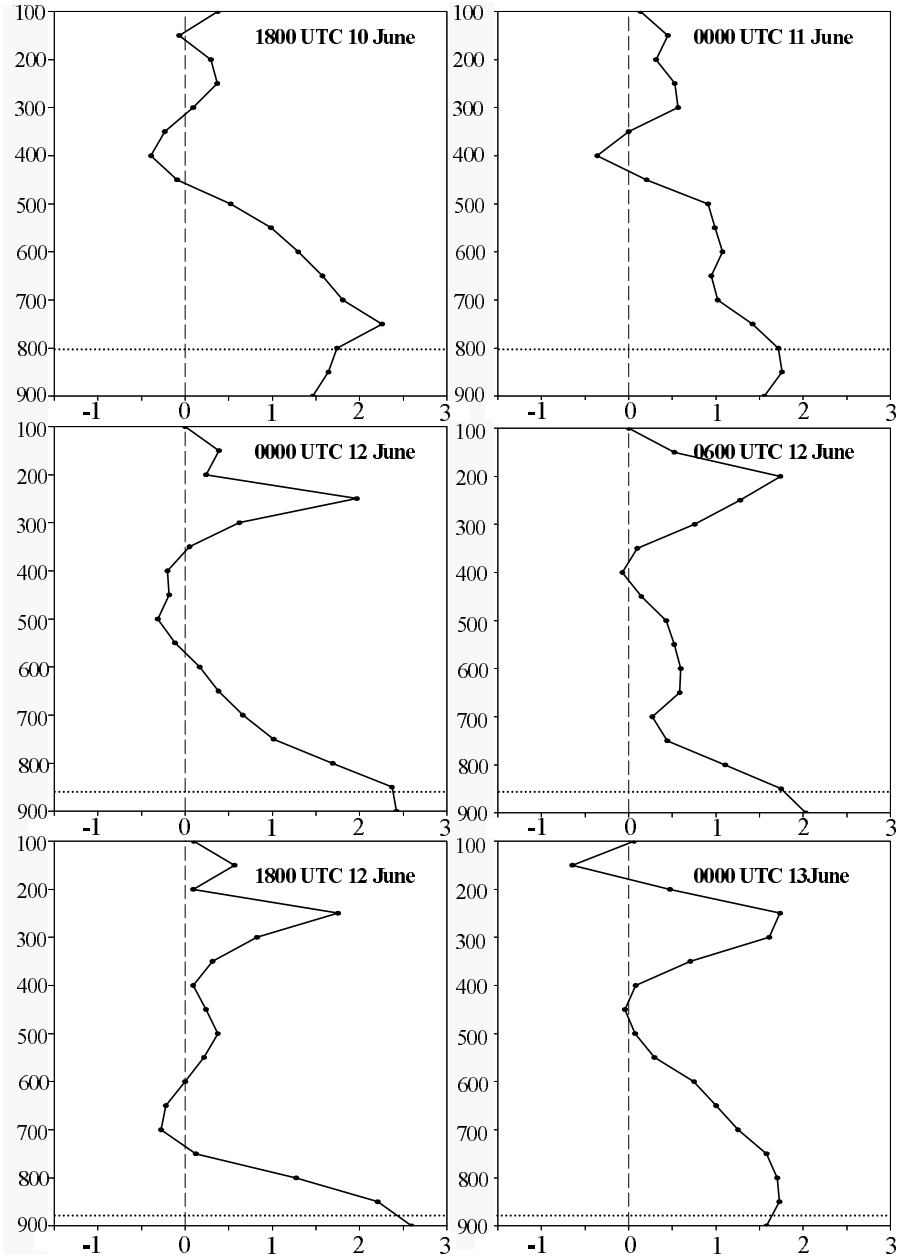

Fig. 8. Area-averaged conversion from APE to divergent wind KE in KAs of the SWV (solid, unit: 10^{-3} J kg^{-1} s^{-1}). Dashed lines represent 0 lines, and dotted lines stand for the representative terrain height in the SWV KAs.

troposphere (Table 1).

When vortex B formed around 0000 UTC 13 June, there was a strong conversion from APE to divergent wind KE in the KA for the development of vortex B, and the negative potential function, upward motion, convergence centers (Fig. 7), and convection (Fig. 3) were enhanced in the KA. The conversion from APE to divergent wind below 500 hPa with a maximum around 800 hPa (Fig. 8) may have impacted upon the maintenance and propagation of vortex B downward to 850 hPa, six hours later. Comparison between Fig. 5 and Fig. 8 reveals a linear relationship, i.e. the bigger the CAD term, the stronger the SP term.

4.2 *APE budget*

The variation of APE was investigated using Eq. (7) and the results are shown in Fig. 9. We defined the term a2+a4 to represent the total effect of vertical motion. Between C1 and C2, the term a1 was positive with a maximum around 400 hPa, which col-

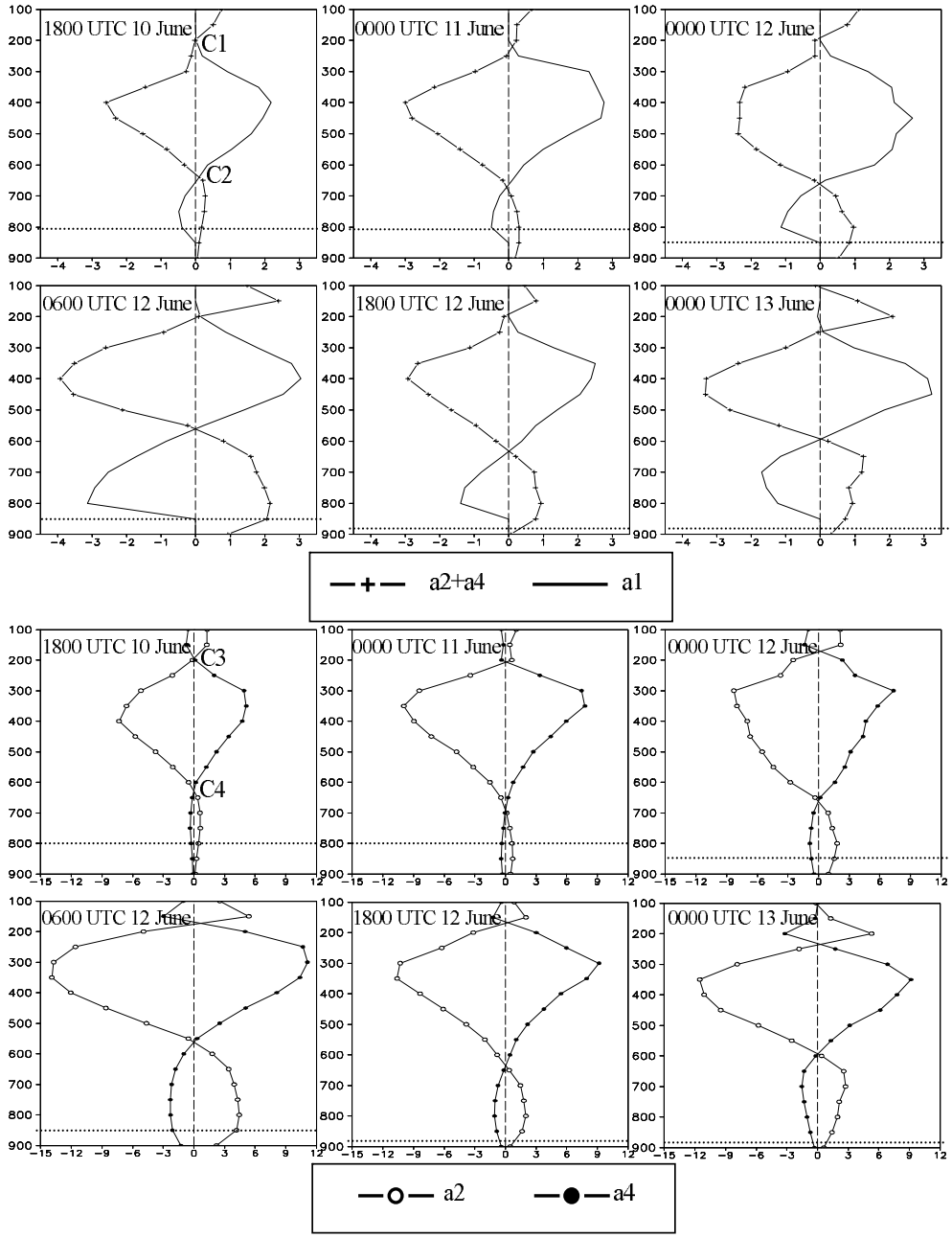

Fig. 9. Area-averaged terms (a1, a2, a4, units: 10^{-3} J kg^{-1} s^{-1}) of APE budget equation in the SWV KAs, where C1–C4 stand for representative intersection of lines, and dotted lines represent terrain height of the SWV KAs.

locates approximately to the maximum latent heat release center. The terms a2 and a4 were approximately axisymmetric. Since the magnitude of the term a2 was larger than that of term a4, the distribution of term a2+a4 was close to that of a2, and their total effect was positive above C1, negative between C1 and C2, and positive below C2. The term a2 was negative between C3 and C4, corresponding to the upward motion associated with the direct thermal circulation. As a result, the vertical motion with the direct thermal circulation caused the release of APE. The term a4 was positive between C3 and C4, due to the horizontal temperature gradient enhancement (not shown). The terms a2 and a4 were roughly axisymmetric. Suppose that a2=−a4; namely,

$$N\omega\alpha = -c_p N\left(-\omega\frac{\partial T}{\partial p}\right) .$$

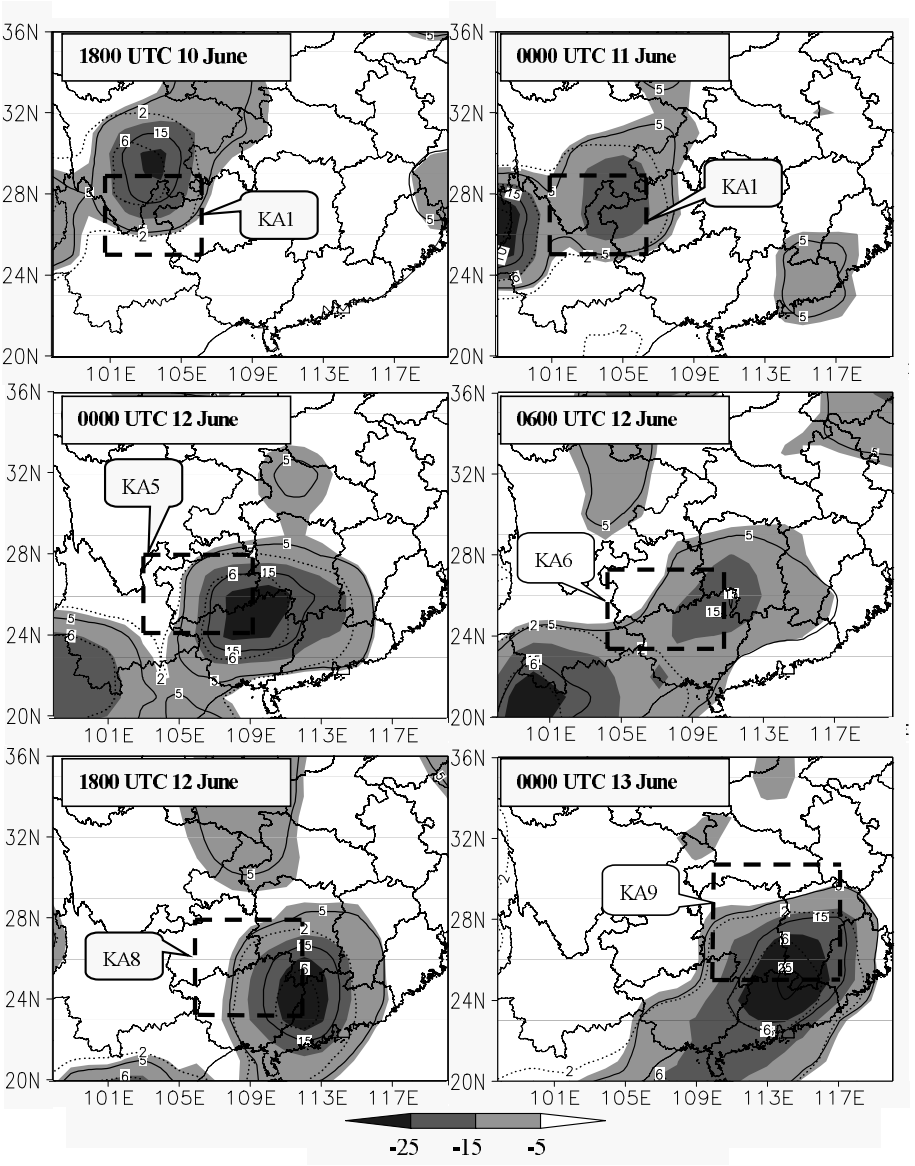

Fig. 10. Integral of APE budget term (a1, a2 and a4) from surface to 100 hPa (units: J m^{-2} s^{-1}), where shaded areas are the integral of term a2, solid lines are the integral of a4, and dotted lines are the integral of a1. Dashed rectangles stand for the SWV KAs.

Substituting $dp/dz = -g/\alpha$ (hydrostatic equation, where p is pressure) into the equation leads to a dry adiabatic lapse rate equation ($dT/dz = -g/c_p$). Thus, if air parcels move with the dry adiabatic lapse rate, the total effect of vertical motion would be zero.

As the effect of temperature advection was much smaller than that of diabatic heating from latent heat release, the term a3 was one order of magnitude smaller than that of a2 or a4,which was mainly favourable for an increase in APE (not shown).

As shown in Fig. 10, during the lifetime of the SWV, there was strong APE generation (terms a1 and a4) and release (term a2), and the centers of the three terms were almost collocated. APE-release zones were consistent with convective activity (Fig. 3), which indicates that APE release was related to strong upward motion and heavy rainfall. Upward motion associated with the direct thermal circulation was very important for APE release (term a2). Diabatic heating from latent heat release and vertical temperature advection were important for APE generation.

The conceptual model shown in Fig. 11 describes the relationships among APE, SWV development, divergent wind KE, rotational wind KE, vertical motion,

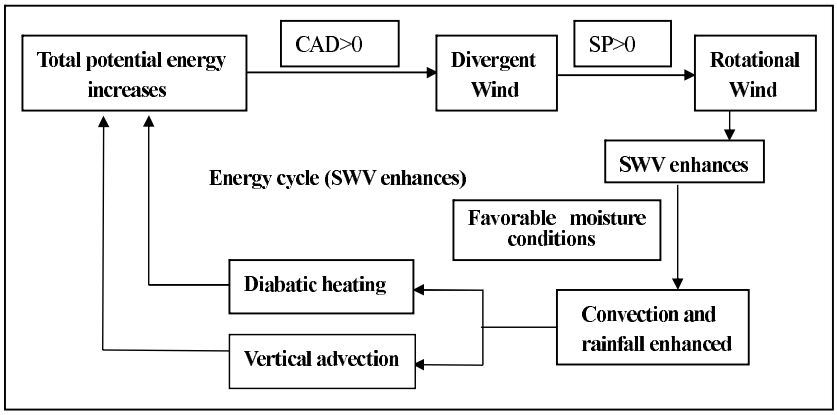

Fig. 11. A conceptual model of the SWV energy conversion.

and diabatic heating. The model envisages that when total potential energy increases, the conversion from APE to divergent wind, as well as the conversion of KE from divergent wind to increased rotational wind, results in the development of the SWV. Under this condition, the vertical motion will be enhanced, and if there is favorable moisture conditions, the latent heat release will also intensify. As a result, the total potential energy will increase through diabatic heating (a1) and vertical advection (a4) (Fig. 11). On the contrary, when direct thermal circulation occurred during the lifetime of the SWV, the total potential energy decreased, and then the conversion from APE to KE of divergent wind weakened, resulting in the conversion of KE from rotational to divergent wind. This leads to a weak SWV.

5. Summary and conclusions

The budgets of KE and APE of an eastward-propagating SWV from 11–13 June 2008 with heavy rainfall over southern China were calculated in order to study the formation, maintenance and dissipating mechanism of the SWV, as well as the relationship between heavy rainfall and the SWV. The main results were:

(1) KE generation and advection were the most important KE sources, while friction and sub-grid processes were the main KE sinks. Rotational and divergent wind KE generation were the most vital factors in the formation of the SWV, while the advection associated with the background circulation dominated during the middle maintenance stage of the SWV and the formation of vortex B.

(2) The downward conversion from divergent to rotational wind KE was consistent with the downward stretching of the SWV. The Coriolis force was very important in the formation and maintenance of the SWV. Convergence was instrumental in the maintenance of the SWV, as well as the formation of vortex B. The vertical motion was unfavorable for the development of the SWV during the formation and maintenance stages, and favorable for the maintenance of the SWV during the mature and vortex B formation stages.

(3) The conversion from APE to KE of divergent wind was an essential process for the generation of KE. Strong convergence resulted in strong conversion, which led to active convection. The conversion of CAD remained strong below 500 hPa, with the maximum moving from the mid to lower troposphere, which was similar to the term SP. The large magnitude of the term CAD was associated with the large magnitude of term SP, indicating that APE was instrumental in the formation and maintenance of the SWV.

(4) The impacts of the dynamical and thermal processes of vertical motion on APE occurred in an opposing fashion. When the air parcels varied with the dry adiabatic lapse rate, the total effect would be zero. In this case, vertical motion with direct thermal circulation was the most vital method of APE release. Latent heat release and vertical temperature advection were conducive for an increase in APE, while horizontal temperature advection influenced APE only slightly.

(5) Based on the above results, a conceptual model of energy conversion during the life cycle of the SWV has been proposed. When conversion from APE to KE of divergent wind and KE from divergent wind to an increase in rotational wind takes place, favorable conditions for the development of the SWV occur. If moisture is abundant, latent heat release will intensify, causing total potential energy to be enhanced by the diabatic heating and vertical advection.

Acknowledgements. This research was supported by the project of the State Key Laboratory of Severe Weather, Chinese Academy of Meteorological Sciences

(Grant No. 2010LASW-A02), National Natural Science Foundation of China (Grant No. 40875021), the project of the National Key Basic Research and Development of China (No. 2009CB421401) and the Chinese Special Scientific Research Project for Public Interest (Grant No. GYHY200906004).

REFERENCES

Chen, S.-J., L.-S. Bai, and E.-C. Kung, 1990: An approach to kinetic energy diagnosis of meso-synoptic scale interaction. *Mon. Wea. Rev.,* **118**, 837–844.

Chen, T.-C., 1980: On the energy exchange between the divergent and rotational components of atmospheric flow over the tropics and subtropics at 200 mb during two northern summers. *Mon. Wea. Rev.,* **108**, 896–912.

Chen, T.-C., and A. Wiin-Nielsen, 1976: On the kinetic energy of divergent and nondivergent flow in the atmosphere. *Tellus,* **28**, 486–498.

Chen, T.-C., J. C. Alpert, and T. W. Schlater, 1978: The effects of divergent and non-divergent winds on the kinetic energy budget of a mid-latitude cyclone: A case study. *Mon. Wea. Rev.,* **108**, 458–468.

Chen, Q.-Z., Y.-W. Huang, Q.-W. Wang, and Z.-M. Tan, 2007: The statistical study of the southwest vortexes during 1990–2004. *Journal of Nanjing University* (*Natural Sciences*), **43**(6), 633–642. (in Chinese)

Chen, S.-J., and D. Lorenzo, 1984: Numerical prediction of the heavy rain vortex over eastern Asia monsoon region. *J. Meteor. Soc. Japan,* **6**(2), 730–747.

Chen, Z.-M., and W.-B. Min, 2000: Statistics analysis of southwest vortex. *The Secondary Proceedings of Qingzang Plateau Meteorology Conference*, 368–378. (in Chinese)

Chen, Z.-M., Q. Miu, and W.-B. Min, 1998: A case analysis on mesoscale structure of severe southwest vortex. *Journal of Applied Meteorological Science*, **9**(3), 273–282. (in Chinese)

Chen, Z.-M., M.-L. Xu, W.-B. Min, and Q. Miu, 2003: Relationship between abnormal activities of southwest vortex and heavy rain the upper reach of Yangtze River during summer of 1998. *Plateau Meteorology*, **22**(2), 162–167. (in Chinese)

Ding, Y.-H., and Y.-Z. Liu, 1985a: On the analysis of typhoon kinetic energy, Part I Budget of total kinetic energy and eddy kinetic energy. *Science in China* (*B*), **15**(10), 957–966. (in Chinese)

Ding, Y.-H., and Y.-Z. Liu, 1985b: On the analysis of typhoon kinetic energy, Part II Conversion between divergent and nondivergent wind. *Science in China* (*B*), **15**(11), 1045–1054. (in Chinese)

Ding, Z.-Y., and J.-K. Chen, 1995: A study of relationship between enhancement of typhoon rain and available potential energy and cold air. *Journal of Tropical Meteorology*, **11**(1), 80–85. (in Chinese)

Dimego, G. J., and L. F. Bosart, 1982: The transformation of tropical storm agnes into an extra-tropical cyclone. *Mon. Wea. Rev.*, **110**(5), 412–430.

Edmon, H. J., Jr., 1978: A reexamination of limited area available potential energy budget equations. *J. Atmos. Sci.*, **35**(9), 1655–1659.

Fu, S.-M., 2009: Study on the structure characteristics and formation mechanism of southwest vortex with heavy rainfall. Ph. D. dissertation, Institute of atmospheric physics, Chinese Academy of Sciences, 211pp. (in Chinese)

Gao, S.-T., 1987: The dynamic action of the disposition of the fluid fields and the topography on the formation of the south-west vortex. *Chinese J. Atmos. Sci.,* **11**(3), 263–271. (in Chinese)

Kuo, H.-L., 1974: Further studies of the parameterization of the influence of cumulus convection on large scale flow. *J. Atmos. Sci.*, **31**, 1232–1240.

Kuo, Y.-H., L.-S. Cheng, and J.-W. Bao, 1988: Numerical simulation of the 1981 Sihuan flood. *Mon. Wea. Rev.,* **1**(16), 2481–2504.

Li, G.-P., B.-J. Zhao, and J.-Q. Yang, 2002: A dynamical study of the role of surface sensible heating in the structure and intensification of the Tibetan Plateau vortices. *Chinese J. Atmos. Sci.*, **26**(4), 519–525. (in Chinese)

Lorenz, E. N., 1978: The available energy and the maintenance of a moist circulation. *Tellus*, **30**, 15–31.

Lu, J.-H., 1986: *Generality of the Southwest Vortex*. China Meteorological Press, Beijing, 1–270. (in Chinese)

Sun, G.-W, and B.-D. Chen, 1994: Characteristics of the lows flocking with Tibet atmospheric low-frequency oscillation over the Qinghai-Xizang (Tibet) Plateau. *Chinese J. Atmos. Sci.,* **18**(1), 113–121. (in Chinese)

Tao, S.-Y., 1980: *Rainstorms in China*. Science Press, Beijing, 225pp. (in Chinese)

Wang, Z., and K. Gao, 2003: Sensitivity experiments of an eastward-moving southwest vortex to initial perturbations. *Adv. Atmos. Sci.,* **20**(4), 638–649.

Wu, G.-X., and H.-Z. Liu, 1999: Complete form of vertical vorticity tendency equation and slantwise vorticitiy development. *Acta Meteorologica Sinica*, **57**(1), 1–15. (in Chinese)

Zhao, S.-X., 1977: Case study of southwest vortex structure. *Proceedings of Qingzang Plateau Meteorology Conference*, Xining, 296–306. (in Chinese)

Zhao, S.-X., and S.-M. Fu, 2007: An analysis on the southwest vortex and its environment fields during heavy rainfall in eastern Sichuan Province and Chongqing in September 2004. *Chinese J. Atmos. Sci.,* **31**(6), 1059–1075. (in Chinese)

Zhu, H., B.-S. Deng, and H. Wu, 2002: The development of southwest vortex in conservation of moist potential vorticity. *Acta Meteorologica Sinica*, **60**(3), 343–351. (in Chinese)